CHEMISTRY
A European Journal

A Journal of
ChemPubSoc Europe

## Accepted Article

**Title:** Tunable Ligand Effects on Ruthenium Catalyst Activity for Selectively Preparing Imines or Amides by Dehydrogenative Coupling Reactions of Alcohols and Amines

**Authors:** Takafumi Higuchi, Risa Tagawa, Atsuhiro Iimuro, Shoko Akiyama, Haruki Nagae, and Kazushi Mashima



**To be cited as:** *Chem. Eur. J.* 10.1002/chem.201701342

**Link to VoR:** http://dx.doi.org/10.1002/chem.201701342

Supported by
ACES

WILEY-VCH

10.1002/chem.201701342

WILEY-VCH

FULL PAPER

# Tunable Ligand Effects on Ruthenium Catalyst Activity for Selectively Preparing Imines or Amides by Dehydrogenative Coupling Reactions of Alcohols and Amines

Takafumi Higuchi, Risa Tagawa, Atsuhiro Iimuro, Shoko Akiyama, Haruki Nagae, and Kazushi Mashima*[a]

**Abstract:** Selective dehydrogenative synthesis of imines from a variety of alcohols and amines was developed using the ruthenium complex $RuCl_2$(dppea)$_2$ (**6a**: dppea = 2-diphenylphosphino-ethylamine) in the presence of catalytic amounts of $Zn(OCOCF_3)_2$ and KO$^t$Bu, while selective dehydrogenative formation of amides from the same sources was achieved using another ruthenium complex, $RuCl_2$((*S*)-dppmp)$_2$ [**6d**: (*S*)-dppmp = (*S*)-2-((diphenyl-phosphenyl)methyl)pyrrolidine], in the presence of catalytic amounts of $Zn(OCOCF_3)_2$ and KHMDS. Our previously reported ruthenium complex, Ru$(OCOCF_3)_2$(dppea)$_2$ (**8a**), was the catalyst precursor for the imine synthesis, while Ru$(OCOCF_3)_2$((*S*)-dppmp)$_2$ (**8d**), which was derived from the treatment of **6d** with $Zn(OCOCF_3)_2$ and characterized by single crystal X-ray analysis, was the pre-catalyst for the amide formation. Control experiments revealed that zinc salt functioned as a reagent for replacing chloride anions with trifluoroacetate anions. Plausible mechanisms for both selective dehydrogenative coupling reactions are proposed based on a time-course study, Hammett plot, and deuterium-labeling experiments.

## Introduction

Catalytic dehydrogenative oxidation of alcohols is a straightforward protocol for the *in situ* generation of carbonyl compounds,[1] whose coupling reactions with amines, alcohols, and alkenes lead to the corresponding C—N,[2] C—O, [2d,3] and C—C[4] bond formations. Such dehydrogenative coupling reactions of alcohols have attracted recent interest from synthetic organic chemists due to their easy accessibility and the ability to use cheap alcohols as starting compounds, as well as their remarkable environmentally benign and atom-economical processes. More precisely, dehydrogenative coupling reactions of alcohols with amines in general gives two products, *i.e.*, imines and amides. As shown in Scheme 1, the first step is the catalytic dehydrogenation of alcohol which affords the corresponding carbonyl compound, *i.e.*, ketone from secondary alcohol and aldehyde from primary alcohol, and a sequential condensation reaction with amines results in the formation of a hemiaminal intermediate. Imine is formed by liberating water from the hemiaminal intermediate (pathway A), while amide is produced by eliminating molecular hydrogen from the same intermediate (pathway B).

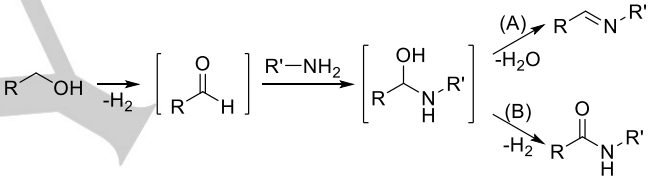


**Scheme 1.** Reaction pathways of dehydrogenative coupling of alcohols and amines.

Some homogeneous catalyst systems have been developed for dehydrogenative coupling reactions of alcohols with amines to predominantly yield the corresponding imines or amides, depending on the choice of a suitable catalyst system of ruthenium, [5,6] rhodium,[7] osmium,[8] cobalt,[9] or manganese.[10] It is a challenging task to develop a catalytic system that can control the selectivity between imine formation and amide by a rather simple modification of the ligand and/or additives to any suitable catalyst precursor. For example, Milstein *et al.* demonstrated that such the selectivity was controlled by altering a side-arm substituent of the ligand skeleton through modifying one of two phosphorus atoms bound to the nitrogen atom; a PNP pincer-ligated ruthenium complex **I** catalyzed the imine selective reaction while a PNN pincer ruthenium complex **II** showed amide selectivity (Scheme 2).[5a,6b] Another unique example was reported by Madsen *et al.,* who used ruthenium catalyst **III** to exclusively produce imine upon adding DABCO and to select for amide by adding both $PCy_3$ and KO$^t$Bu (Scheme 3).[5c,6c]

With our continuing interest in controlling such selectivity, we recently found that a suitable substituent on the skeleton of the nitrogen atom of the P—N chelating ligand bound to the ruthenium atom led to the selective production of imines or amides. We thus applied new ruthenium catalyst systems to the selective formation of imines and amides with a wide substrate scope, and propose plausible mechanisms for the selective

[a] T. Higuchi, R. Tagawa, Dr. A. Iimuro, S. Akiyama, Dr. H. Nagae, Prof. Dr. K. Mashima
Department of Chemistry, Graduate School of Engineering Science
Osaka University
Toyonaka, Osaka, 560-8531 (Japan)
E-mail: mashima@chem.es.osaka-u.ac.jp

Supporting information for this article is given via a link at the end of the document.

dehydrogenative coupling reaction based on controlled experiments.

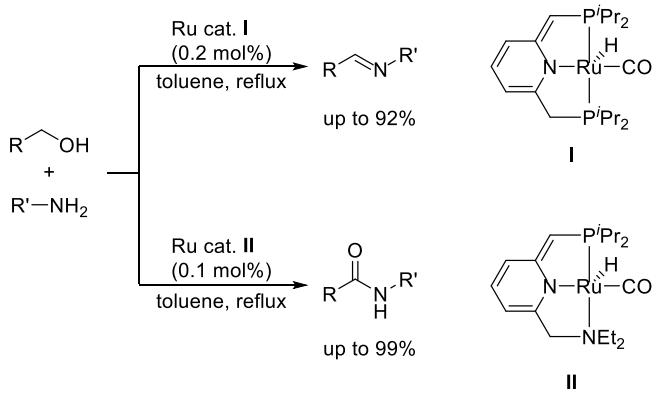


**Scheme 2.** Selective dehydrogenative coupling reactions of alcohols and amines by choosing ruthenium catalysts **I** and **II**.[5a,6b]

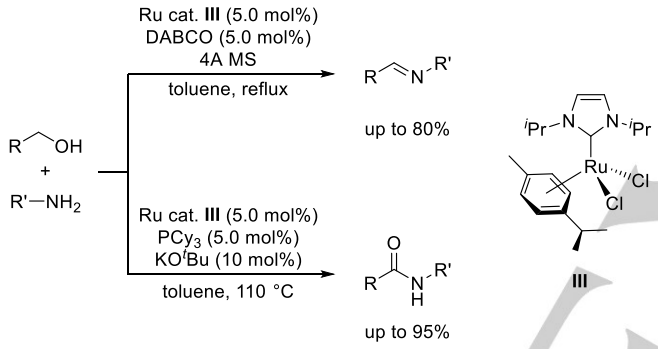


**Scheme 3.** Selective dehydrogenative coupling reactions of alcohols and amines by choosing additives.[5c,6c]

## Results and Discussion

We began by searching for ruthenium catalysts that assisted the dehydrogenative coupling reaction of alcohols and amines, for which we tested several ruthenium complexes that are catalysts capable of reducing carbonyl compounds, the inverse of the alcohol dehydrogenation reaction. Benzyl alcohol (**1a**) and *n*-hexylamine (**2a**) were selected as model substrates under catalytic conditions of ruthenium complexes (1.0 mol%) and KO$^t$Bu (20 mol%) in 1,4-dioxane at refluxing temperature for 18 h, and the results are summarized in Table 1. Complex $RuCl_2(dppea)_2$ (**6a**: dppea = 2-diphenylphosphinoethylamine) produced an imine **3aa** as the major product (60%) along with a homo-coupling product **4aa** (12%) and an amide **5aa** (4%) (entry 1). The use of a longer chained P—N ligand, dpppa (dpppa = 3-diphenylphosphinopropylamine), decreased the yield of **3aa** and increased the yield of **5aa** (entry 2). A ruthenium complex with a bulky ligand, d$^t$bpea (d$^t$bpea = 2-di(*tert*-butyl)phosphino-ethylamine), in which two *tert*-butyl groups were bound to the phosphorus atom, resulted in a decreased yield of **3aa** (entry 3). Bidentate phosphine ligand dppe gave only 7% **3aa** (entry 5). The combination of P—P and N—N ligands on the ruthenium centre did not work effectively (entry 6), indicating that the P—N ligand played an important role. When a tridentate phosphine ligand, triphos (triphos = 1,1,1-tris(diphenyl-phosphinomethyl)ethane), was used, only **3aa** was obtained with a low yield (entry 7). Accordingly, **6a** was chosen as the best catalyst for imine-synthesis. On the other hand, the ruthenium complex **6d** bearing (*S*)-dppmp [(*S*)-dppmp = (*S*)-2-((diphenylphosphenyl)methyl)-pyrrolidine] surprisingly exhibited a different selectivity for producing amide **5aa** in 69% yield (entry 4). Thus, **6d** was selected as a catalyst for amide synthesis.

**Table 1.** Screening of catalysts for dehydrogenative coupling of **1a** and **2a**.

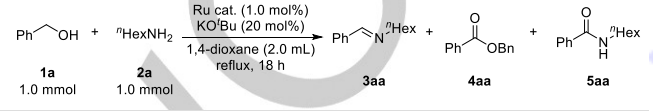


| entry | Ru cat. | Yield (%)[a] 3aa | 4aa | 5aa |
|---|---|---|---|---|
| 1 | $RuCl_2(dppea)_2$ (**6a**) | 60 | 12 | 4 |
| 2 | $RuCl_2(dpppa)_2$ (**6b**) | 57 | 13 | 11 |
| 3 | $RuCl_2(d^tbpea)_2$ (**6c**) | 45 | 6 | 10 |
| 4 | $RuCl_2((S)\text{-dppmp})_2$ (**6d**) | 1 | n.d. | 69 |
| 5 | $RuCl_2(dppe)_2$ (**6e**) | 7 | n.d. | n.d. |
| 6 | $RuCl_2(dppp)(dpen)$ (**6f**) | 8 | 1 | 21 |
| 7 | $[Ru_2(triphos)_2(\mu\text{-}Cl)_3]Cl$ (**6g**) | 17 | n.d. | n.d. |

[a] The yields were determined by GC analysis using dodecane as an internal standard.

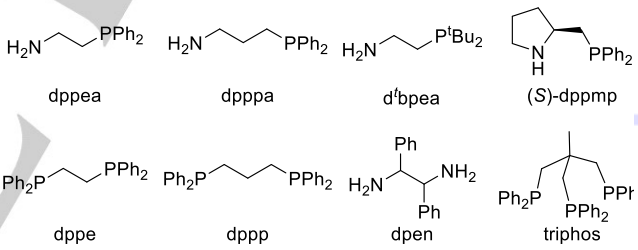


**Optimization of catalytic conditions using 6a for dehydrogenative imine synthesis**

Because **6a** worked as a catalyst for dehydrogenative imine formation, we tuned the catalytic conditions of the bases and solvents. Among organic and inorganic bases such DBU, KO$^t$Bu, KHMDS, NaOMe, $NaHCO_3$, and $K_2CO_3$, we selected KO$^t$Bu as the best base (Table S1). Using **6a** (1.0 mol%) and KO$^t$Bu (20 mol%) under refluxing conditions for 18 h, we tested ethereal solvents such as 1,4-dioxane, THF, and CPME; a protic solvent, $^t$BuOH; non-polar solvents, such as toluene and hexane; and DCE, and we found that 1,4-dioxane was the best solvent for dehydrogenative imine synthesis (Table S2). We then examined the additive effects of Lewis acids as it was anticipated that imine formation would be accelerated by activating the expected dehydrated intermediate of aldehyde with Lewis acids, and the results are shown in the supporting information, Table S3.[11] We selected $Zn(OCOCF_3)_2$ as the best Lewis acid. Under these catalytic conditions, we tuned the ratio of the substrates and catalyst loadings. Finally, 50% excess alcohol **1a** and 0.5 mol%

10.1002/chem.201701342





of **6a** were selected as the optimized conditions (Table 2, entry 1; Table S4).

**Time-course study for dehydrogenative synthesis of imine 3aa**

Figure 1 shows the time-course product distribution among **3aa**, **4aa**, and **5aa**. Although the amount of imine **3aa** increased over time, only trace amounts of ester **4aa** and amide **5aa** were present, suggesting that **4aa** and **5aa** were not produced prior to **3aa**. Notably, benzaldehyde was not observed at all during the reaction course, indicating that under the reaction conditions, *in situ*-generated aldehyde was rapidly liberated from the catalytic centre followed by the reaction with amine.

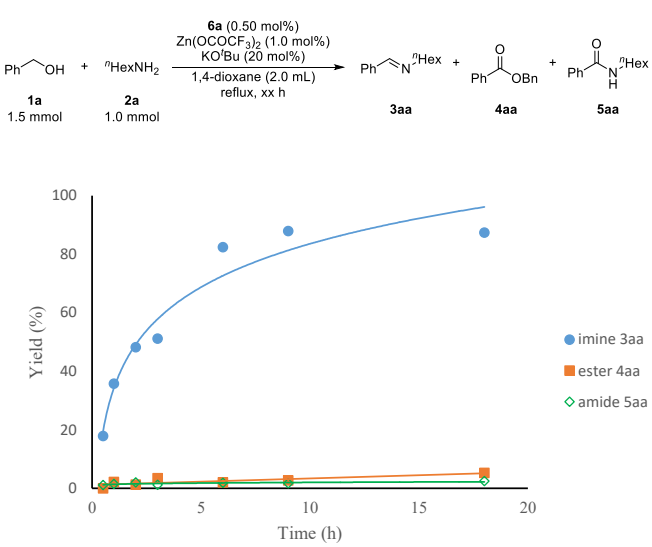


**Figure 1.** Time-course study of the dehydrogenative imine synthesis.

**Substrate scope for dehydrogenative synthesis of imine**

With the optimized conditions in hand, we evaluated the substrate scope for imine synthesis, and the results are shown in Tables 2 and 3. Table 2 shows the reaction of *n*-hexylamine (**2a**) with various alcohols. Excellent to good yields were obtained when electron-rich (methoxy and methyl)-substituted benzyl alcohols were used (entries 2—5). Bromo and chloro substituents at the *para* position of the phenyl group were tolerated to give a moderately high yield of the corresponding imine (entries 6 and 7). Electron-deficient benzyl alcohol (**1h**) gave a relatively lower yield compared with electron-rich benzyl alcohol (entry 8). Alkyl alcohols were applicable to this system affording excellent to good yields (entries 9—11). The presence of the *N*-heteroaromatic moiety of alcohol **1l** did not retard the dehydrogenative coupling reaction (entry 12).

**Table 2.** Substrate scope of dehydrogenative imine synthesis (alcohols).

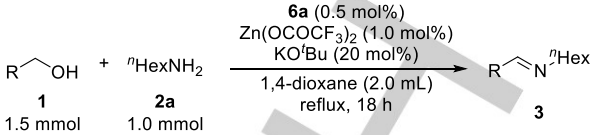


| Entry | Alcohol | | Imine | | Yield (%)[a] |
|---|---|---|---|---|---|
| 1 | 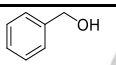 | **1a** | 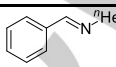 | **3aa** | 83 (81) |
| 2 | 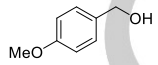 | **1b** | 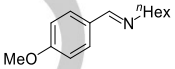 | **3ba** | 95 (73) |
| 3 | 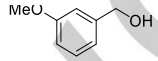 | **1c** | 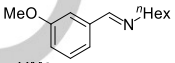 | **3ca** | 83 (79) |
| 4 | 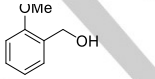 | **1d** | 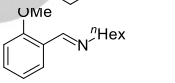 | **3da** | 70 (52) |
| 5 | 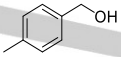 | **1e** | 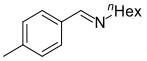 | **3ea** | 86 (88) |
| 6 | 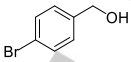 | **1f** | 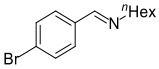 | **3fa** | 73 (74) |
| 7 | 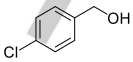 | **1g** | 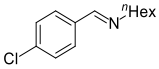 | **3ga** | 79 (81) |
| 8 | 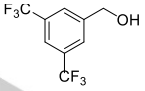 | **1h** | 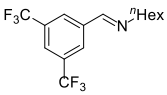 | **3ha** | 43 (43) |
| 9 | 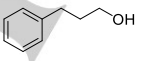 | **1i** | 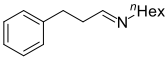 | **3ia** | 76 (42) |
| 10[b] | 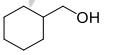 | **1j** | 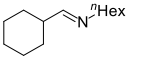 | **3ja** | 91 (63) |
| 11 | 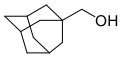 | **1k** | 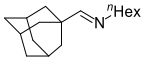 | **3ka** | 72 (60) |
| 12 | 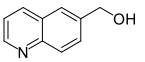 | **1l** | 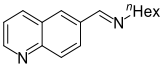 | **3la** | 73 (74) |

[a] The yield was determined by $^1$H NMR analysis with *N*-methylbenzamide as an internal standard. The isolated yield is given in parentheses. [b] *N*-methylcyclohexanecarboxamide was used as an internal standard.

Reaction of benzyl amine (**2b**) with benzyl alcohol (**1a**) under the optimized conditions using **6a** as the catalyst gave the corresponding imine **3ab** in good yield (Table 3, entry 1). Cyclohexylamine (**2c**) was converted into imine **3ac** in moderate yield, whereas a bulky alkyl amine, 1-aminoadamantane (**2d**), drastically retarded imine formation (entries 2 and 3). Internal amino alcohol **2e** converted into the corresponding imine, which was isomerized to indole (**3e**) (entry 4). In contrast to alkyl amines, aniline (**2f**) and its derivatives (**2g**—**2l**) exhibited different reactivity. In the reaction of aniline, an almost 1:1 ratio of the corresponding imine **3af** and amine **7af** were obtained (entry 5). The yields of *N*-(methoxyphenyl)-1-phenylmethan-imine **3ag**—**3ai** changed independently of the position of the methoxy group; the *para* position gave mainly corresponding imine **3ag** while the *meta* methoxy moiety **2h** was converted into imine **3ah** and amine **7ah** in almost the same yields, and amine **7ai** was the major product afforded using *ortho* methoxy aniline (**2i**) (entries 6—8). Reaction with *para* methylaniline (**2j**) gave a mixture of imine and

10.1002/chem.201701342





amine, while reaction with *ortho* methylaniline (**2k**) gave mainly imine (entries 9 and 10). 4-Bromo aniline could be applied to this system (entry 11), and the conformation of imine **3al** was the *E* form as confirmed by X-ray diffraction study (Figure S3, Supporting Information).

**Table 3.** Substrate scope of dehydrogenative imine synthesis (amines).

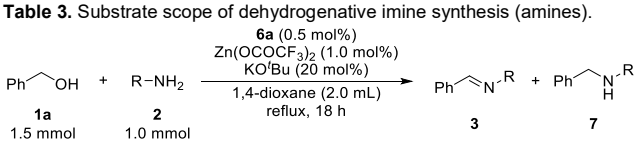


**1a** 1.5 mmol; **2** 1.0 mmol; **3**; **7**

| Entry | Amine | | Imine | | Yield (%)[a] |
|---|---|---|---|---|---|
| 1 | 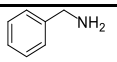 | **2b** | 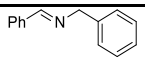 | **3ab** | 88 (70) |
| 2 | 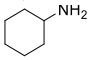 | **2c** | 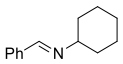 | **3ac** | 63 (51) |
| 3 | 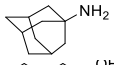 | **2d** | 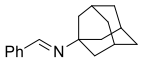 | **3ad** | 15 (9) |
| 4 | 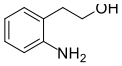 | **2e** |  | **3e** | 96 (91) |
| 5 | 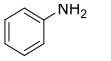 | **2f** | 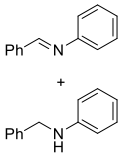 | **3af**<br>**7af** | 43 (23)<br>54 (40) |
| 6 | 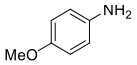 | **2g** | 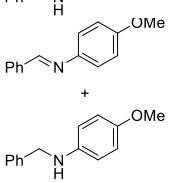 | **3ag**<br>**7ag** | 80 (65)<br>20 (17) |
| 7 | 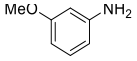 | **2h** | 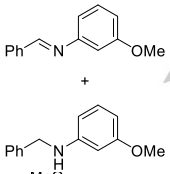 | **3ah**<br>**7ah** | 47 (40)<br>53 (60) |
| 8 | 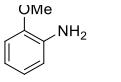 | **2i** | 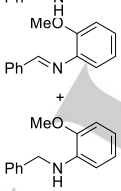 | **3ai**<br>**7ai** | 28 (11)<br>64 (63) |
| 9 | 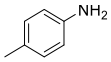 | **2j** | 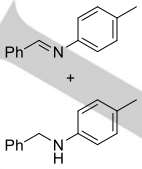 | **3aj**<br>**7aj** | 54 (45)<br>35 (17) |
| 10 | 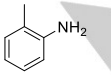 | **2k** | 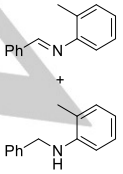 | **3ak**<br>**7ak** | 80 (65)<br>16 (7) |
| 11 | 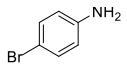 | **2l** | 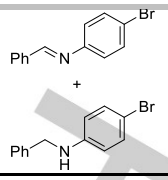 | **3al**<br>**7al** | 25 (12)<br>74 (79) |

[a] The yield was determined by $^1$H NMR analysis with *N*-methylbenzamide as an internal standard. The isolated yield is given in parentheses. [b] 1.0 mol% of [Ru] and 2.0 mol% of [Zn] were used.

## Optimization of catalytic conditions using complex 6d for dehydrogenative amide synthesis

We searched for a suitable base and solvent for dehydrogenative synthesis of amide upon using **6d** (1.0 mol%). Among the organic and inorganic bases examined, such as DBU, KO$^t$Bu, KHMDS, NaOMe, $NaHCO_3$, and $K_2CO_3$, we selected KHMDS as the best (Table S5). After evaluating the mixture of **6d** (1 mol%) and KHMDS (20 mol%) for 18 h in appropriate solvents such as 1,4-dioxane, THF, CPME, $^t$BuOH, toluene, hexane, and DCE, we selected CPME as the best solvent for dehydrogenative amide synthesis (Table S6). We then examined the additive effects of Lewis acids (Table S7), and $Zn(OCOCF_3)_2$ was chosen as the best additive. Under these catalytic conditions, we tuned the ratio of substrates and catalyst loadings, and, finally, 50% excess *n*-hexylamine **2a** and 1.0 mol% of **6d** were selected as the optimized conditions (Table 4, entry 1; Table S8).

## Time-course study for dehydrogenative synthesis of amide 5aa

The product distribution among **3aa**, **4aa**, and **5aa** was examined, and the time-course is shown in Figure 2. The yield of amide **5aa** was high in the early stage, while only trace amounts of imine **3aa** and ester **4aa** were detected. Aldehyde was an expected intermediate, but it was not detected throughout the reaction.

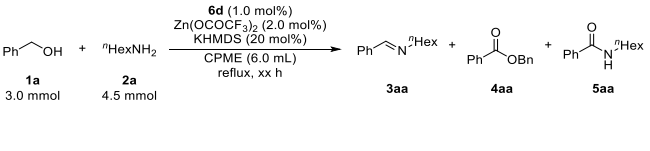


**1a** 3.0 mmol; **2a** 4.5 mmol; **3aa**; **4aa**; **5aa**

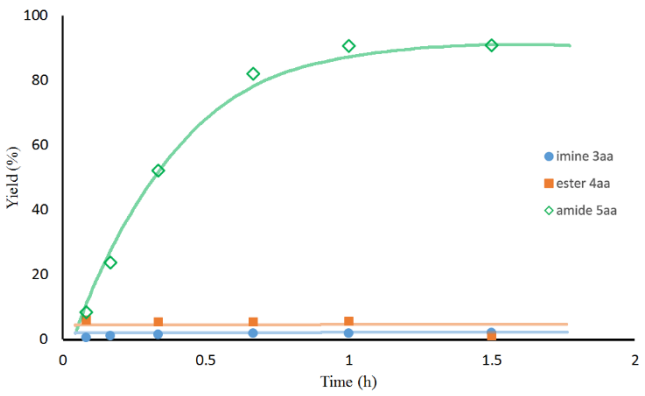


**Figure 2.** Time-course study of the dehydrogenative amide synthesis.

10.1002/chem.201701342



# FULL PAPER

**Substrate scope for dehydrogenative synthesis of amide**

We explored the substrate scope of alcohols and amines for amide synthesis (Tables 4 and 5). Electron-rich benzyl alcohol, methoxy benzyl alcohol (**1b**—**1d**) and 4-methyl benzyl alcohol (**1e**), formed corresponding amide **5ba**—**5ea** in high yield (entries 2—5). Benzamide bearing a halogen atom at the *para* position on the benzene ring, bromo (**5fa**) and chloro (**5ga**) groups, was obtained in 83% yield, respectively (entries 6 and 7). A 21% yield of **5ha** was obtained using alcohol **1h** bearing a strong electron-withdrawing group (entry 8). Primary alcohol (**1i**) was effectively converted into amide **5ia** compared with sterically hindered alcohols (**1j** and **1k**) (entries 9—11). 6-Quinolinemethanol (**1l**) was converted into the corresponding amide with a hydrogenated quinoline skeleton (entry 12).[12]

**Table 4.** Substrate scope of dehydrogenative amide synthesis (alcohols).

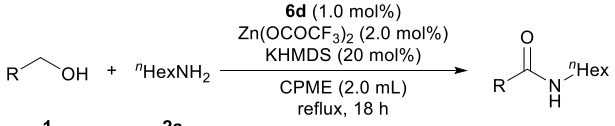


| Entry | Alcohol | | amide | | Yield (%)[a] |
|---|---|---|---|---|---|
| 1 |  | **1a** | 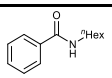 | **5aa** | 86 |
| 2 | 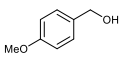 | **1b** | 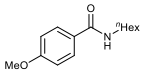 | **5ba** | 90 |
| 3 | 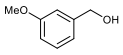 | **1c** | 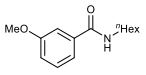 | **5ca** | 87 |
| 4 |  | **1d** | 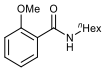 | **5da** | 83 |
| 5 |  | **1e** | 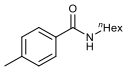 | **5ea** | 90 |
| 6 | 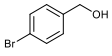 | **1f** | 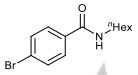 | **5fa** | 83 |
| 7 | 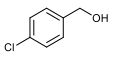 | **1g** | 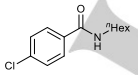 | **5ga** | 83 |
| 8 | 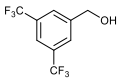 | **1h** | 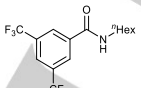 | **5ha** | 21 |
| 9 | 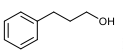 | **1i** | 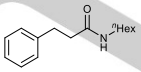 | **5ia** | 58 |
| 10 |  | **1j** | 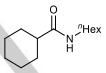 | **5ja** | 23 |
| 11 | 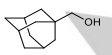 | **1k** | 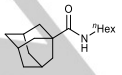 | **5ka** | 8 |
| 12 | 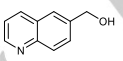 | **1l** | 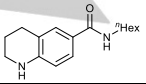 | **5la** | 27 |

[a] Isolated yield.

*N*-benzyl benzamide (**5ab**) was obtained in high yield (Table 5, entry 1). Cyclohexyl-amine (**2c**) retarded the reaction and 1-amino adamantane (**2d**) showed no reaction (entries 2 and 3). Lower reactivity was observed when aniline (**2f**) was used (entry 4) and other aniline derivatives also exhibited low reactivity. Methyl-protected amino ethanol (**2m**) could be applied for this system (entry 5). Tertiary amides **5an** and **5ao** were obtained using morpholine (**2n**) and 3,5-dimethylpiperidine (**2o**) as amine sources (entries 6 and 7). The five-membered ring amine **2p** was converted into the corresponding tertiary amide **5ap** in a higher yield than a six-membered ring amine (entries 7 vs. 8). An unsymmetrical secondary amine, such as benzyl methyl amine (**2q**) was less reactive than primary amine (entry 9). 2-Aminophenyl-ethanol (**2e**) was converted into indole (**3e**), while we expected that 2-aminophenyl-ethanol (**2e**) would form indoline-2-one in this system (entry 10).

**Table 5.** Substrate scope of dehydrogenative amide synthesis (amines).


| Entry | Amine | | amide | | Yield (%)[a] |
|---|---|---|---|---|---|
| 1 |  | **2b** | 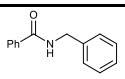 | **5ab** | 86 |
| 2 |  | **2c** | 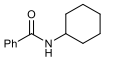 | **5ac** | 58 |
| 3 |  | **2d** | 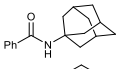 | **5ad** | Not obtained |
| 4 |  | **2f** | 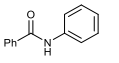 | **5af** | 13 |
| 5 |  | **2m** | 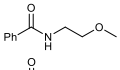 | **5am** | 81 |
| 6 |  | **2n** | 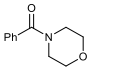 | **5an** | 66 |
| 7 |  | **2o** | 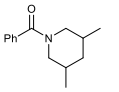 | **5ao** | 68 |
| 8 |  | **2p** |  | **5ap** | 76 |
| 9 |  | **2q** |  | **5aq** | 24 |
| 10 |  | **2e** |  | **3e** | 76 |

[a] Isolated yield.

**Synthesis and characterization of $Ru(OCOCF_3)_2(dppea)_2$ (8a) and $Ru(OCOCF_3)_2((S)\text{-dppmp})_2$ (8d)**

Because $Zn(OCOCF_3)_2$ acts as a superior additive to $RuCl_2(L)_2$ [**6a**: L = dppea; **6d**: L = (*S*)-dppmp], we conducted the reaction of $Zn(OCOCF_3)_2$ with **6d**, though we previously reported $Ru(OCOCF_3)_2(dppea)_2$ (**8a**) as a product of $Zn(OCOCF_3)_2$ with

10.1002/chem.201701342





**6a**.[13] $Ru(OCOCF_3)_2$((*S*)-dppmp)$_2$ (**8d**) was obtained by treating **6d** with $Zn(OCOCF_3)_2$ in the presence of KHMDS (eq. 1). The structural features of complex **8d** were determined by $^{19}F\{^1H\}$ and $^{31}P\{^1H\}$ NMR analysis along with an X-ray diffraction study. The $^{19}F\{^1H\}$ NMR spectrum of **8d** displayed one singlet signal assignable to trifluoroacetate ligand at -74.7 ppm, which is similar to the signal of complex **8a**. The signal of phosphorus atom at 52.5 ppm was observed on $^{31}P\{^1H\}$ NMR analysis in contrast to complex **8a** at 62.0 ppm, indicating that the conformations of the ligands differed. Figure 3 shows the crystal structure of **8d** together with that of **8a** (Figure 4) as a comparison. Both trifluoroacetate ligands on **8d** coordinated in a $\eta^1$ fashion to the ruthenium atom, the same as **8a**. The trifluoroacetate ligands in **8d** occupy the *trans* position, in sharp contrast to the *cis* configuration of the two trifluoroacetate ligands in **8a**. Hence, each phosphorous atom of two P—N chelating ligands were located next to each other, and each phosphorus atom was placed at a *trans* position to each nitrogen atom, in contrast to the case of **8a** in which each phosphorus atom was *trans* to the oxygen atom of trifluoroacetate.

$RuCl_2$((*S*)-dppmp)$_2$ (**6d**) —[$Zn(OCOCF_3)_2$ (2.0 equiv.), KHMDS (2.0 equiv.), CPME, 100 °C, 12 h]→ $Ru(OCOCF_3)_2$((*S*)-dppmp)$_2$ (**8d**, 69% yield) (1)

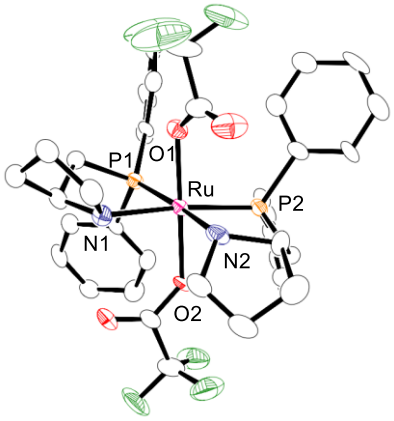


**Figure 3.** ORTEP drawing of $Ru(OCOCF_3)_2$((*S*)-dppmp)$_2$ (**8d**). All hydrogen atoms are omitted for clarity.

**Table 6.** Selected bond distances (Å) and angles (deg.) of complex **8d**.

| | | | |
|---|---|---|---|
| Ru—P1 | 2.280(3) | Ru—N2 | 2.184(1) |
| Ru—P2 | 2.249(3) | P1—Ru—P2 | 103.7(4) |
| Ru—O1 | 2.112(9) | N1—Ru—N2 | 90.0(4) |
| Ru—O2 | 2.109(9) | O1—Ru—O2 | 178.3(3) |
| Ru—N1 | 2.225(1) | | |

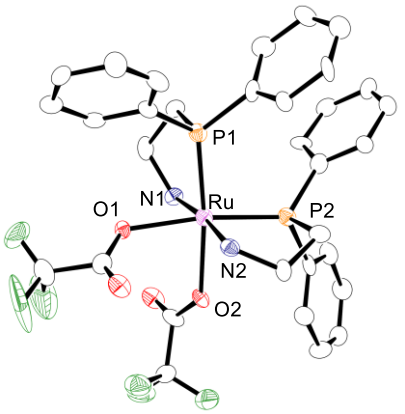


**Figure 4.** ORTEP drawing of $Ru(OCOCF_3)_2$(dppea)$_2$ (**8a**).[13] All hydrogen atoms are omitted for clarity.

**Mechanistic studies of catalytic dehydrogenative coupling reactions of benzyl alcohol (1a) and *n*-hexylamine (2a), producing the corresponding imine 3aa by 8a and amide 5aa by 8d.**

First, we checked the catalytic activities of the isolated ruthenium complexes **8a** and **8d**. Notably, the complex **8a** became a catalyst for the dehydrogenative reaction of benzyl alcohol (**1a**) and *n*-hexylamine (**2a**) in the presence or absence of $Zn(OCOCF_3)_2$ to yield imine **3aa** in almost the same yields (89% and 87% yields, respectively) (eq. 2), indicating that the trifluoroacetate ligand played an important role in this reaction and $Zn(OCOCF_3)_2$ acted as a reagent for replacing chloride anions by trifluoroacetate anions. Similarly, **8d** afforded amide **5aa** in the same high yield with or without $Zn(OCOCF_3)_2$ (eq. 3).

Ph—CH$_2$OH (**1a**, 1.5 mmol) + $^n$HexNH$_2$ (**2a**, 1.0 mmol) —[**8a** (0.5 mol%), $Zn(OCOCF_3)_2$ (xx mol%), KO$^t$Bu (20 mol%), 1,4-dioxane (2.0 mL), reflux, 18 h]→ Ph—CH=N—$^n$Hex (**3aa**) (2)

| xx = | 0 | 1.0 |
|---|---|---|
| | 89% | 87% |

Ph—CH$_2$OH (**1a**, 1.0 mmol) + $^n$HexNH$_2$ (**2a**, 1.5 mmol) —[**8d** (1.0 mol%), $Zn(OCOCF_3)_2$ (xx mol%), KHMDS (20 mol%), CPME (2.0 mL), reflux, 18 h]→ Ph—C(=O)—N(H)—$^n$Hex (**5aa**) (3)

| xx = | 0 | 2.0 |
|---|---|---|
| | 92% | 92% |

With catalyst **8a** for *the dehydrogenative imine synthesis*, we measured the relative reaction rates of *n*-hexyl amine (**2a**) with *p*-substituted benzyl alcohols **1** with electronic variation (Figure 5). A Hammett plot of the initial rates in a short reaction time (3 h) provided the $\rho$ value (−0.28) for $\log k_{rel}$ ($k_{rel} = k_X/k_H$) versus $\sigma^+$, indicating that electron-withdrawing substituents retarded the dehydrogenative imine synthesis, and the rate-determining transition state can be assumed to be stabilized by electron-donating substituents (*vide infra*: transition state **A** in Figure 6).[14] Moreover, a deuterium-labeling study was conducted using

10.1002/chem.201701342





benzyl alcohol-α,α-$d_2$ (**1a**-$d_2$), giving the kinetic isotope effect (KIE = 1.45). In addition, molecular hydrogen was detected by $^1$H NMR analysis by the dehydrogenative imine synthesis from benzyl alcohol (**1a**) and *n*-hexylamine (**2a**) in a sealed NMR tube. Based on the Hammett plot and the deuterium-labeling experiment, C—H (C—D) bond cleavage was assumed to be the turnover-over limiting step. Because basic additive was indispensable for this imine synthesis (Table S1), the base was assumed to induce deprotonation of one of two protons at the $NH_2$ moiety of the ligand on **8a** to generate the ruthenium-amido complex **8a'**, which works as a catalytically active species to oxidize alcohol to aldehyde *via* transition state **A** (Figure 6, outer-sphere Noyori-type transition state).[15]

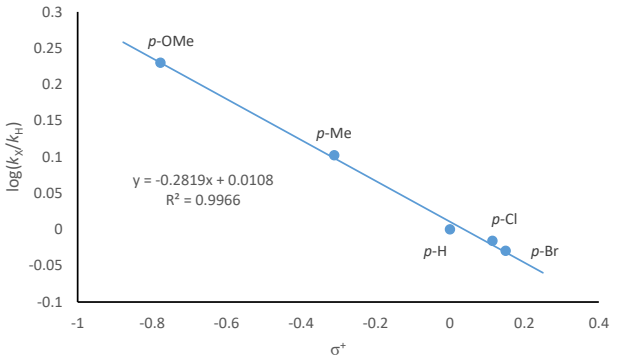


**Figure 5.** Hammett Plot for the dehydrogenative imine synthesis.

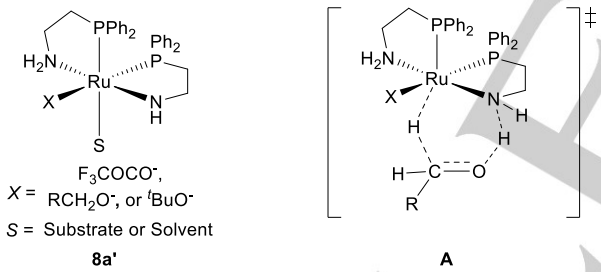


**Figure 6.** Proposed structure of complex **8a'** and **A**.

Isolated complex **8d** was used for *the dehydrogenative synthesis of amides*. The dehydrogenative coupling reaction tended to proceed without any hydrogen acceptors,[6a,6d,6j,7a] which are often essential reagents; molecular hydrogen was observed, however, in the amide synthesis of benzyl alcohol (**1a**) and *n*-hexylamine (**2a**) in a sealed NMR tube. The relative rates were measured for the reactions of *n*-hexyl amine (**2a**) with *p*-substituted benzyl alcohols **1** with electronic variation. Figure 7 shows a Hammett plot of the initial rates in a short reaction time (2 h) at 80 ºC, which clearly indicating a non-linear free energy relationship. Thus, it is assumed that the rate-determining transition state does not involve alcohol substrates.[14] Moreover, an *inverse* secondary kinetic isotope effect (KIE = 0.83) was observed in a deuterium labeling study for benzyl alcohol-α,α-$d_2$ (**1a**-$d_2$), consistent with the fact that C—H (C—D) bonds showed rehybridization of the $sp^2$-carbonyl carbon of aldehyde to $sp^3$-hemiaminal carbon in the turnover limiting step[16] Thus, we expected that the turnover-limiting step was a nucleophilic attack of an amine to an aldehyde bound to the ruthenium center, in which we proposed aldehyde-ruthenium complex **B** as an intermediate (Figure 8) because a dissociated aldehyde was immediately reacted with the amine to give the corresponding imine as mentioned in Figure 1. The reactivity to give amide is probably due to the pyrrolidine moiety on the (*S*)-dppmp ligand which is bulkier than the $NH_2$ moiety on the dppea ligand.[6b,17]

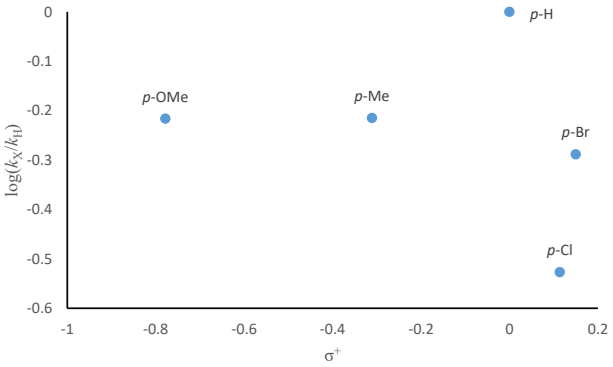


**Figure 7.** Hammett Plot for the dehydrogenative amide synthesis.

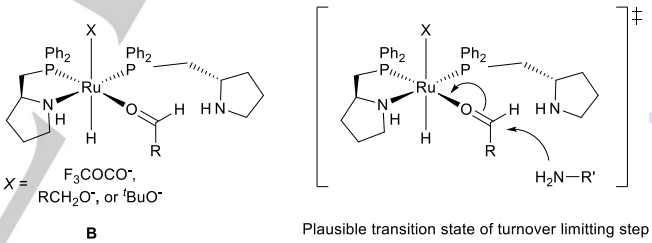


**Figure 8.** Proposed structure of complex **B** and transition state of turnover limiting step.

## Conclusions

In conclusion, we report a ligand-controlled selective dehydrogenative coupling reaction of alcohols and amines to give the corresponding imines or amides catalyzed by ruthenium complexes bearing P—N ligand with zinc salts. A wide variety of alcohols and amines were used in the present systems to obtain the corresponding imines and amides. A new ruthenium complex **8d** was successfully synthesized and fully characterized. Isolated complexes **8a** and **8d** exhibited catalytic activity for dehydrogenative imine or amide synthesis, respectively. Moreover, we propose these reaction mechanisms based on our experiments, including a time-course study, Hammett plot, and measurements of the kinetic isotope effect. The bulkiness of pyrrolidine moiety of the (*S*)-dppmp plays an important role in the hemi-labile ligation for the selective dehydrogenative amide synthesis, while imine was selectively obtained using dppea as a ligand that does not dissociate from the ruthenium centre.

## Experimental Section

### General Information

All manipulations involving air- and moisture-sensitive compounds were carried out under an argon atmosphere by using standard vacuum line and Schlenk tube techniques. All liquid alcohols and amines were distilled under an argon atmosphere from the calcium hydride. Alternatively, toluene, THF, $Et_2O$ and hexane were dried and deoxygenated by using Grubbs column (Glass Counter Solvent Dispending System, Nikko Hansen & Co, Ltd.). 1,4-Dioxane was distilled over sodium benzophenone ketyl under an argon atmosphere. Amide substrates were synthesized by standard condensation reaction of acyl chlorides and amines. All other reagents were purchased at the highest commercial quality and used without further purification. Flash column chromatography was performed using silica gel 60 (0.040–0.063 mm, 230–400 mesh ASTM).

### Physical Measurements

$^1$H NMR (400 MHz), $^{13}$C{$^1$H} NMR (100 MHz), $^{19}$F{$^1$H} NMR (376 MHz) and $^{31}$P{$^1$H} NMR (160 MHz) spectra were measured on Bruker Avance III-400 spectrometers in 5 mm NMR tubes. All $^1$H NMR chemical shifts were reported in ppm relative to the residual solvent protons in chloroform-$d_1$ at δ 7.26, benzene-$d_6$ at δ 7.16, dichloromethane-$d_2$ at δ 5.32, and DMSO-$d_6$ at δ 2.50. All $^{13}$C{$^1$H} NMR chemical shifts were reported in ppm relative to carbon resonance of the solvent itself in chloroform-$d_1$ at δ 77.16, benzene-$d_6$ at δ 128.06, dichloromethane-$d_2$ at δ 53.84, and DMSO- $d_6$ at δ 39.52. All $^{19}$F{$^1$H} NMR chemical shifts were reported in ppm relative to an external reference of $\alpha,\alpha,\alpha$-trifluorotoluene at δ -63.9. $^{31}$P{$^1$H} NMR chemical shifts were recorded in ppm relative to 85% $H_3PO_4$ as an external standard at δ 0.00. GC analyses were recorded on a Shimadzu GC-2014 gas chromatograph with J&W Scientific DB-5 column. High-resolution mass spectrometry (HRMS) was performed on a JEOL JMS-700 (EI, FAB plus) and a Brucker Daltonics MicroTOF (ESI plus). IR spectra were recorded on a JASCO FT/IR-230 spectrometer. X-ray crystallographic studies were performed on Rigaku XtaLAB P200 system with graphite-monochromated Mo Kα radiation (λ = 0.71075). All melting point were recorded on BUCHI melting point M-565. Elemental analyses were recorded by using Perkin-Elmer 2400 at the Faculty of Engineering Science, Osaka University.

### General Procedures for the Catalytic Dehydrogenative Coupling Reaction

Dehydrogenative synthesis of imine: A mixture of $RuCl_2$(dppea)$_2$ (**6a**) (dppea = 2-diphenylphosphinoethane; 3.2 mg, 5.0 X $10^{-3}$ mmol), $Zn(OCOCF_3)_2$ (2.9 mg, 1.0 X $10^{-2}$ mmol), KO$^t$Bu (22.4 mg, 0.20 mmol), alcohol (1.5 mmol), and amine (1.0 mmol) in 1,4-dioxane (2.0 mL) was refluxed for 18 h. After cooling to room temperature, the resulting mixture was purified by silica gel column chromatography (Hexane:$NEt_3$ = 20:1).

Dehydrogenative synthesis of amide: A mixture of $RuCl_2$((*S*)-dppmp)$_2$ (**6d**) [(*S*)-dppmp = (*S*)-2-((diphenylphosphanyl)methyl)-pyrrolidine; 7.1 mg, 1.0 X $10^{-2}$ mmol], $Zn(OCOCF_3)_2$ (5.8 mg, 2.0 X $10^{-2}$ mmol), KHMDS (39.9 mg, 0.200 mmol), alcohol (1.0 mmol), and amine (1.5 mmol) in CPME (2.0 mL) was refluxed for 18 h. After cooling to room temperature, the resulting mixture was purified by silica gel column chromatography (Hexane:AcOEt = 8:1).

### Synthetic Procedure of Complexes

Complexes **6a**,[19] **6b**,[20] **6d**,[21] **6e**,[22] **6f**,[23] **6g**,[24] and **8a**[13] were synthesized according to literature procedures.

Synthesis of $Ru(OCOCF_3)_2$((*S*)-dppmp)$_2$ (**8d**)

CPME (3.0 mL) was added to a mixture of $RuCl_2$((*S*)-dppmp)$_2$ (**6d**) (71.1 mg, 0.100 mmol), $Zn(OCOCF_3)_2$ (58.3 mg, 0.200 mmol), and KHMDS (39.9 mg, 0.200 mmol) at room temperature. The orange reaction mixture was stirred at 100 °C for 13 h. All volatiles were removed *in vacuo* to give brown solid. The solid was extracted by $Et_2O$ (5 mL X 3) and filtered through the pad of Celite. The filtrate was concentrated to obtain yellow solid (60 mg, 0.069 mmol, 69% yield). Mp 218 °C (dec.); $^1$H NMR (400 MHz, benzene-$d_6$, 30 °C), δ 1.33-1.57 (m, 4H, *methylene*), 1.61-1.82 (m, 4H, *methylene*), 2.35-2.53 (m, 2H, *methylene*), 2.61-2.79 (m, 4H, *methylene*), 2.79-2.95 (m, 2H, *methylene*), 3.90 (br s, 2H, *methyne*), 6.80-7.08 (m, 16H, *Ar*), 7.31 (br s, 4H, *Ar*), 8.40 (br s, 2H, N*H*); $^{13}$C{$^1$H} NMR (100 MHz, benzene-$d_6$, 30 °C) δ 27.7, 31.4$_7$ (d, $J_{C\text{-}P}$ = 7.7 Hz), 31.5$_4$ (d, $J_{C\text{-}P}$ = 7.7 Hz), 37.4 (d, $J_{C\text{-}P}$ = 14 Hz), 37.6 (d, $J_{C\text{-}P}$ = 14 Hz), 48,5, 59.8 (d, $J_{C\text{-}P}$ = 2.4 Hz), 59.8 (d, $J_{C\text{-}P}$ = 2.4 Hz), 114.3 (q, $J_{C\text{-}F}$ = 292 Hz), 129.4, 130.1, 132.5 (d, $J_{C\text{-}P}$ = 4.4 Hz), 132.6 (d, $J_{C\text{-}P}$ = 4.4 Hz), 133.5 (d, $J_{C\text{-}P}$ = 4.9 Hz), 133.6 (d, $J_{C\text{-}P}$ = 4.9 Hz), 166.7 (q, $J_{C\text{-}F}$ = 36 Hz), two aryl signals were overlapped with signal of deuterium solvent; $^{19}$F{$^1$H} NMR (376 MHz, benzene-$d_6$, 30 ºC) δ -74.7; $^{31}$P{$^1$H} NMR (162 MHz, benzene-$d_6$, 30 ºC) δ 52.5; IR (KBr, ν/cm$^{-1}$) 3443, 3179, 3059, 2963, 1686, 1670, 1486, 1435, 1415, 1261, 1198, 1137, 1099, 1026, 839, 803, 788, 741, 727, 696, 527, 513; MS (FAB) m/z 866 ($M^+$); HRMS (FAB) m/z calcd. for $C_{38}H_{40}F_6N_2O_4P_2Ru$ 866.1411 found 866.1404; Anal. Calcd for $C_{38}H_{40}F_6N_2O_4P_2Ru$: C, 52.72; H, 4.66; N, 3.24. Found: C, 52.56; H, 4.95; N, 2.89.

## Acknowledgements

T.H. and A.I. acknowledge financial support from a JSPS Research Fellowship for Young Scientists and the JSPS Japanese-German Graduate Externship Program. This work was supported by JSPS KAKENHI Grant Number JP15H057950, a Grant-in-Aid for Scientific Research on Innovative Areas, and JP262480280, a Grant-in-Aid for Scientific Research(A) of The Ministry of Education, Culture, Sports, Science, and Technology, Japan. We thank Prof. H. Tsurugi and Dr. Y. Kita for fruitful discussions.

**Keywords:** dehydrogenative synthesis • ruthenium • imine • amide • selectivity

[1] J. March, Advanced Organic Chemistry, sixth ed.; Wiley: New York, **1992**.

[2] a) M. H. S. A. Hamid, P. A. Slatford, J. M. J. Williams, *Adv. Synth. Catal.* **2007,** *349,* 1555. b) G. E. Dobereiner, R. H. Crabtree, *Chem. Rev.* **2010,** *110,* 681. c) G. Guillena, D. J. Ramon, M. Yus, *Chem. Rev.* **2010,** *110,* 1611. d) C. Gunanathan, D. Milstein, *Science* **2013,** *341,* 249. e) C. Chen F. Verpoort, Q. Wu, *RSC Adv.* **2016,** *6,* 55599. f) Q. Yang, Q. Wang, Z. Yu, *Chem. Soc. Rev.* **2015,** *44,* 2305.

[3] a) S. Tang, J. Yuan, C. Liu, A. Lei, *Dalton Trans.* **2014,** *43,* 13460. b) I. B. Krylov, V. A. Vil', A. O. Terent'ev, *Beilstein J. Org. Chem.* **2015,** *11,* 92.

[4] a) J. M. Ketcham, I. Shin, T. P. Montgomery, M. J. Krische, *Angew. Chem., Int. Ed.* **2014,** *53,* 9142. b) A.-M. J. Dechert-Schmitt, D. C. Schmitt, T. Itoh, M. J. Krische, *Nat. Prod. Rep.* **2014,** *31,* 504. c) K. D. Nguyen, B. Y. Park, T. Luong, H. Sato, V. J. Garza, M. J. Krische, *Science* **2016,** *354,* 6310.

[5] a) B. Gnanaprakasam, J. Zhang, D. Milstein, *Angew. Chem., Int. Ed.* **2010,** *49,* 1468. b) J. W. Rigoli, S. A. Moyer, S. D. Pearce, J. M. Schomaker, *Org. Biomol. Chem.* **2012,** *10,* 1746. c) A. Maggi, R. Madsen, *Organometallics* **2012,** *31,* 451. d) B. Saha, S. M. W. Rahaman, P. Daw, G. Sengupta, J. K. Bera, *Chem.—Eur. J.* **2014,** *20,* 6542.

[6] a) T. Naota, S.-I. Murahashi, *Synlett* **1991,** 693. b) C. Gunanathan, Y. Ben-David, D. Milstein, *Science* **2007,** *317,* 790. c) L. U. Nordstrøm, H. Vogt, R. Madsen, *J. Am. Chem. Soc.* **2008,** *130,* 17672. e) A. J. A. Watson, A. C. Maxwell, J. M. J. Williams, *Org. Lett.* **2009,** *11,* 2667. f) Y. Zhang, C. Chen, S. C. Ghosh, Y. Li, S. H. Hong, *Organometallics* **2010,** *29,* 1374. g) J. H. Dam, G. Osztrovszky, L. U. Nordstrøm, R. Madsen, *Chem.—Eur. J.* **2010,** *16,* 6820. j) N. D. Schley, G. E. Dobereiner, R. H. Crabtree, *Organometallics* **2011,** *30,* 4147. k) X. Xie, H. V. Huynh, *ACS Catal.* **2015,** *5,* 4143. j) K. Kim, B. Kang, S. H. Hong, *Tetrahedron* **2015,** *71,* 4565. k) T. T. Nguyen, K. L. Hull, *ACS Catal.* **2016,** *6,* 8214.

[7] a) T. Zweifel, J.-V. Naubron, H. Grützmacher, *Angew. Chem., Int. Ed.* **2009,** *48,* 559. (b) S. C. Ghosh,; S. Muthaiah, Y. Zhang, X. Xu, S. H. Hong, *Adv. Synth. Catal.* **2009,** *351,* 2643.

[8] M. A. Esteruelas, N. Honczek, M. Oliván, E. Oñate, M. Valencia, *Organometallics* **2011,** *30,* 2468.

[9] G. Zhang, S. K. Hanson, *Org. Lett.* **2013,** *15,* 650.

[10] A. Mukherjee, A. Nerush, G. Leitus, L. J. W. Shimon, Y. Ben-David, N. A. E. Jalapa, D. Milstein, *J. Am. Chem. Soc.* **2016,** *138,* 4298.

[11] a) R. D. Patil, S. Adimurthy, *Asian J. Org. Chem.* **2013,** *2,* 726. b) W. Qin, S. Long, M. Panunzio, S. Biondi, *Molecules* **2013,** *18,* 12264.

[12] Reduction of quinoline catalyzed by ruthenium complex, see; a) Y. Watanabe, T. Ohta, Y. Tsuji, T. Hiyoshi, Y. Tsuji, *Bull. Chem. Soc. Jpn.* **1984,** *57,* 2440. b) Y.-G. Zhou, X.-W. Han, S.-M. Lu, *J. Organomet. Chem.* **2007,** *692,* 3065. c) G. I. Nikonov, V. H. Mai, *Organometallics* **2016,** *35,* 943.

[13] Y. Kita, T. Higuchi, K. Mashima, *Chem. Commun.* **2014,** *50,* 11211.

[14] H. M. Yau, A. K. Croft, J. B. Harper, *Chem. Commun.* **2012,** *48,* 8937.

[15] a) K.-J. Haack, S. Hashiguchi, A. Fujii, T. Ikariya, R. Noyori, *Angew. Chem., Int. Ed.* **1997,** *36,* 285. b) R. Noyori, S. Hashiguchi, *Acc. Chem. Res.* **1997,** *30,* 97. c) S. E. Clapham, A. Hadzovic, R. H. Morris, *Coord. Chem. Rev.* **2004,** *248,* 2201. d) S. M. Joseph, J. S. Samec, J.-E. Backvall, P. G. Andersson, *Chem. Soc. Rev.* **2006,** *35,* 237. e) O. Eisenstein, R. H. Crabtree, *New J. Chem.* **2013,** *37,* 21.

[16] M. Gomez-Gallego, M. A. Sierra, *Chem. Rev.* **2011,** *111,* 4857.

[17] a) V. F. Kuznetsov, G. P. A. Yap, H. Alper, *Organometallics* **2001,** *20,* 1300. b) D. G. Gusev, *ACS Catal.* **2016,** *6,* 6967.

[18] A. Nova, D. Balcells, N. D. Schley, G. E. Dobereiner, R. H. Crabtree, O. Eisenstein, *Organometallics* **2010,** *29,* 6548.

[19] J. M. John and S. H. Bergens, *Angew. Chem., Int. Ed.,* **2011,** *50,* 10377.

[20] L. Saudan, P. Dupau, R. Jean-Jacques and P. Wyss, US20080071121 A1, 2008.

[21] W. Kuriyama, Y. Ino and O. Ogata, US 2010/006394 A1, 2010.

[22] M. A. Fox, J. E. Harris, S. Heider, V. Perez-Gregorio, M. E. Zakrzewska, J. D. Farmer, D. S. Yufit, J. A. K. Howard and P. J. Low, *J. Organomet. Chem.,* **2009,** *694,* 2350.

[23] E. Lindner, A. H. Mayer, I. Warad and K. Eichele, *J. Organomet. Chem*., **2003,** *665,* 176.

[24] E. Iengo, E. Zangrando, E. Baiutti, F. Munini and E. Alssio, *Eur. J. Inorg. Chem.,* **2005,** 1019.

10.1002/chem.201701342

WILEY-VCH



**Entry for the Table of Contents** (Please choose one layout)

Layout 1:

## FULL PAPER

Text for Table of Contents

((Insert TOC Graphic here: max. width: 5.5 cm; max. height: 5.0 cm))

*Author(s), Corresponding Author(s)**

***Page No. – Page No.***

**Title**

Layout 2:

## FULL PAPER

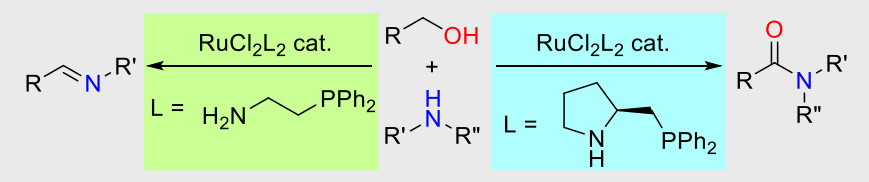


*Author(s), Corresponding Author(s)**

***Page No. – Page No.***

**Title**

Tunable ligand effects on ruthenium catalyst activity for selective synthesis of imines and amides by dehydrogenative coupling reaction is reported.